Research Article

Journal of Applied Material Science & Engineering Research

Freeze-Thaw Characteristics of Water-Based Copper Oxide Nanofluid

Bhaskar C Sahoo[1], Dustin R Ray[1] and Debendra K Das[2*]

[1]*Graduate Student, College of Engineering and Mines, University of Alaska Fairbanks, USA*

[2]*Professor, College of Engineering and Mines, University of Alaska Fairbanks, USA*

[*]Corresponding author

Debendra K Das, College of Engineering and Mines, University of Alaska Fairbanks, P.O. Box 755905, Fairbanks, AK, 99775-5905, USA, Tel: 907-474-6094; Fax: 907-474-6141; E-mail: dkdas@alaska.edu

Submitted: 24 Feb 2018; **Accepted**: 06 Mar 2018; **Published**: 22 Mar 2018

Abstract

This research examined the freeze-thaw characteristics of a water-based copper oxide (CuO) nanofluid for its successful application in cold regions, where freezing of heat transfer fluids can occur. The enhanced thermal conductivity (k) of nanofluid makes it valuable as a heat transfer fluid, but k diminishes as the average particle size (APS) of the dispersed nanoparticles grows. Therefore, experiments were conducted to determine the effect of freezing on the APS of nanofluid suspensions due to agglomeration. Additionally, it was studied, if the freezing point of the nanofluid was elevated or depressed as the volumetric concentration of nanoparticles in the suspension was increased from 1 % to 5%. Another objective of this experimental study was to compare the time required for precooling, freezing and subcooling of different concentrations of nanofluids and the base fluid. The results showed that the APS grew by as much as 51.2% larger due to the phenomenon of freezing, which would reduce the heat transfer performance. The addition of nanoparticles did not affect the freezing point of the nanofluids, tested for two particle volumetric concentrations of 1 and 5 %. It was observed that the precooling time of 5% CuO concentration was the longest. For the complete solidification process, the water and 1% CuO had comparable freezing times, while the 5% nanofluid had the shortest freezing time. The subcooling time was increased with particle volumetric concentration.

Keywords: Agglomeration, concentration, copper oxide, freezing point, freeze-thaw, nanofluid, nanoparticles, solidification, Thermal conductivity

Introduction

Nanofluids are dispersions of nano-scale particles (e.g. copper oxide, aluminum oxide and silicon dioxide etc.) suspended in conventional heat transfer fluids such as water, ethylene or propylene glycol.

Nanofluids have shown to have higher thermal conductivity than the base fluids without the nanoparticles [1]. This enhancement of thermal conductivity increases the convective heat transfer coefficient. The laws of heat transfer dictate that a fluid with high thermal conductivity would greatly enhance the efficiency of heat exchangers. In cold regions of the world, the hydronic heating coils are extensively used as heat exchangers for building heating as described by McQuiston et al [2]. Research conducted by Strandberg and Das on air coils and base board heaters have shown that nanofluids enhance the thermal performance of building heating systems [3,4]. Therefore, nanofluids are desirable candidates for building energy systems, especially in the arctic and subarctic regions, where the heating season may last up to 8 months in a year. Another application of nanofluids is in automobiles, which require heat transfer fluid to serve as engine coolant. Ray and Das studied ethylene glycol based nanofluids as potential candidates for heat transfer in engine cooling applications [5]. In extreme cold climates, nanofluids in automobile radiators or heating coils of a building are susceptible to freezing, due to the sub-zero ambient temperature. Hence studying the characteristics of freezing and thawing of nanofluids has become important for avoiding freeze related failure of heat transfer systems in cold climates.

Presently, the main challenge for nanofluids to become an efficient heat transfer fluids is to achieve stable suspensions over a considerable period of time. To the best of our knowledge no reliable data is available on the effect of freezing on the particle size. In other words it is not known if there is any agglomeration of nanoparticles transforming them to microparticles due to freezing. Hong and Marquis stated that agglomeration leads to change in thermal properties of the nanofluids, because the nanoparticles gradually separate from the base fluid [6]. Many models including those of Chon et al., Koo and Kleinstreuer show that as the particle size increases the thermal conductivity of nanofluids decreases [7,8]. Boutine reported that nanoparticles have about 20% of their atoms near the surface facilitating the transfer of heat efficiently [9]. On the other hand microparticles have most of their atoms far beneath the surface, where they are unable to transfer heat efficiently. Therefore, if the agglomeration of nanoparticles leads to the formation of microparticles, then the efficiency of heat transfer of nanofluids will diminish. Smaller nanoparticle size results in greater surface area for the same volumetric concentration and hence increased heat

transfer. In cold region applications, nanofluids may undergo one or more freeze-thaw cycles and it is desirable to study the effect of such cycles on agglomeration in terms of particle size. From their research on freezing of nanofluids prepared from carbon nanotubes (CNT) in an antifreeze coolant, Hong and Marquis have shown that inclusion of nanoparticles lowered the freezing point of the base fluid [6]. The carbon nanotubes are cylindrical in shape with a high aspect ratio (length/diameter). Carbon nanotubes possess much higher thermal conductivity in the axial direction in comparison to the radial direction. However, nanoparticles are quite different from the CNTs.

Ivall et al. studied the freezing characteristics of CNT nanofluid droplets by cooling it on cold plates and observing the freezing front with respect to time [10]. They found the freezing front velocity varied strongly with freezing rate and concentration.

Limited research has been undertaken on nanoparticles in liquids. Therefore, it is desirable to conduct freeze-thaw experiment with commercially available nanoparticles, which are approximately spherical in shape with an aspect ratio of nearly unity and does not possess directional thermal conductivity.

A property influencing the freezing of nanofluids is its thermal diffusivity. It is defined as $\alpha = k/ p\, c_p$ where k is the thermal conductivity, p is the density and c_p is the specific heat of the fluid. With an increase in the volumetric concentration of nanoparticles, k increases, p increases and c_p decreases. Due to different amount of increase or decrease in these properties with concentration, it is uncertain to predict, if the thermal diffusivity will increase or decrease. Based on the effect of this property alone, nanofluid may cool faster or slower due to increase or decrease of α respectively. Another factor is the thermophoretic force, which acts on nanoparticles in the opposite direction of the temperature gradient. During the radially inward freezing process in a cylindrical pipe in hydronic heating system, this force would push the particles toward the center promoting agglomeration.

In recent years, books have been written on thermophysical properties and various aspects of nanofluids [11,12]. But, not much research has been conducted on the freeze-thaw characteristics of nanofluids. One earlier study on the freezing aspect of aluminum oxide nanofluid has been reported by Maré et al. Research on freezing and thawing characteristics of single phase liquid, mostly on water, have been discussed extensively by Lunardini [13,14]. An equation to predict the time of freezing for water in a cylindrical insulated metal pipe is available from ASHRAE and is listed below [15].

$$t = \rho_l c_{pl} \pi \left(\frac{D_i^2}{2}\right) R_T ln\left[\frac{T_i - T_a}{T_f - T_a}\right] \quad (1)$$

$$R_T = R_c + R_g \quad (2)$$

$$R_c = \frac{1}{h_T \pi D_o} \quad (3)$$

$$R_g = \frac{ln(D_o / D_i)}{2\pi k_g} \quad (4)$$

Although, the thermal resistance due to the glass was negligible (R_c / $R_g \approx 75.5$) c g R R it was accounted for.

Another equation is the Plank's equation [16]. The equation is used to predict freezing time.
Various researchers have used/modified Plank's equation to help in predicting freezing time for various foods [17, 18]. This paper uses the Plank's equation (Eq. (5)) with the modified shape factors presented by Celand and Earle [18].

$$t = \frac{\rho_s h_f}{T_f - T_a}\left(\frac{P \cdot D_i}{h_T} + \frac{R \cdot D_i^2}{k_s}\right) \quad (5)$$

$$P = 0.3751 + 0.099Pk + Ste\left(0.4008Pk + \frac{0.0710}{Bi} - 0.5865\right) \quad (6)$$

$$R = 0.0133 + Ste \cdot (0.0415Pk + 0.3957) \quad (6b)$$

$0.155 \le Ste \le 0.345$; $0.5 \le Bi \le 4.5$; $0 \le Pk \le 0.55$

Where the Biot Number (Eq. (7)), Plank Number (Eq.(8)) and Stefan Number (Eq.(9)) are described below.

$$Bi = \frac{h_T D_i}{k_s} \quad (7)$$

$$Pk = \frac{c_{pl}(T_i - T_f)}{h_f} \quad (8)$$

$$Ste = \frac{c_{ps}(T_f - T_a)}{h_f} \quad (9)$$

When water is frozen the water molecules form an open-cage structure with lots of empty space, thus reducing the density of ice by 10% compared to water [19]

As water freezes (slowly) dissolved and solid particles are not included in the crystalline structure. This is seen with icebergs and glaciers, which are formed from relatively pure water. [20]

There is a difference between saline water and nanofluids, because metallic nanoparticles such as Al_2O_3, CuO and etc. are not dissolved particles such as salt particles in saline water. Therefore, the freeze-thaw characteristics would be different between the nanofluids and the saline water.

From the literature review we find that the freeze-thaw characteristics of nanofluids have not been thoroughly investigated. Addition of nanoscale particles and their resulting Brownian motion will make it different from the freeze-thaw of single phase pure liquids.

As discussed earlier, the main challenge for nanofluids to become successful as efficient heat transfer fluids is to become stably suspended. Nanoparticles in liquids, when subjected to freeze-thaw, tend to agglomerate, resulting in bigger size particles, which will have a tendency to settle.

Agglomeration leads to change in thermal conductivity of the nanofluids. Also, it is well known that particle size significantly

affects the thermal conductivity and thereby the performance of nanofluids. Larger nanoparticle size in nanofluids of equal concentration results in lower particle numbers and less surface area and hence diminished heat transfer performance. In cold region applications, nanofluids may have to be thawed following a freeze up resulting from the heating systems failure for reuse. Therefore, it is desirable to study the effect of such events on agglomeration of particles. It was decided to study the freeze-thaw characteristics of 1 and 5% volumetric concentration CuO nanoparticles dispersed in research grade deionized (D.I.) water.

This experimental investigation was planned to study the freeze-thaw characteristics of CuO nanoparticles dispersed in research grade deionized water. The objectives of this investigation were carefully chosen to answer the following questions: (1) Do nanofluids precool, freeze and subcool at different rates than the base fluids? (2) What effect does concentration have on cooling rate of nanofluids? (3) Does addition of nanoparticles lower the freezing point of nanofluids as in the case of saline water? (4) Do nanoparticles agglomerate due to the freezing? This effect was to be determined from particle size measurements before and after the freeze-thaw cycle?

Materials and Methods

Nanofluid Preparation

The original nanofluid was procured from Alfa Aesar as a 50% (by mass) aqueous suspension of copper oxide (CuO) nanoparticles having an average particle size (APS) of 29nm [21]. Diluted suspensions of 1% and 5% particle concentration (by volume) of the nanofluid were prepared from the original nanofluid by adding pure laboratory grade deionized water. The newly prepared samples were sonicated in a Bransonic B-22 ultrasonicator for 1 hour 30 minutes , based on our past observation, to break agglomerated particles formed due to the gravitational settling [22].

Experimental Setup

The sonicated nanofluid in a laboratory beaker of 500 ml capacity was placed inside the Thermotron 3800 Programmable Temperature chamber with the ambient temperature set to 263.15K [23]. The beaker was insulated from the top and bottom to prevent axial heat flow and ensure radial freezing of the nanofluid. The experimental setup is shown in Figure 1. Twenty-nine (29) copper-constantan thermocouples, distributed along two diametric cross-sections (AA' and BB'), were immersed in the nanofluid. The thermocouples were connected to a National Instruments Inc. data logger and temperature data was collected at every 10-second interval through the Labview software [24,25].

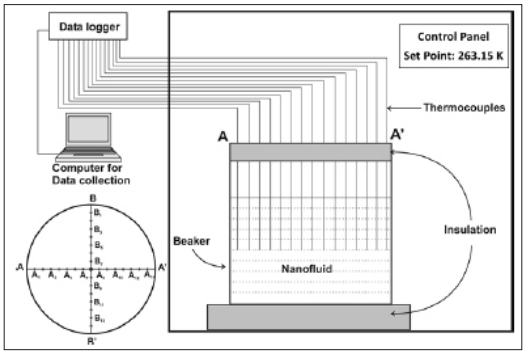

Figure 1: Experimental setup to study the freeze-thaw characteristics of the CuO nanofluid. Notations Ai and Bi represent locations of 29 copper-constantan thermocouples.

Two volumetric concentrations of the CuO nanofluid were used in this experiment (i.e. 1% and 5%) along with the base fluid (water). The samples were in the thermal chamber for nearly 14 hours, where the ambient temperature was set to 263.15 K. Following that, the samples were left to thaw at room temperature (about 293.15 K) for another 24 hours. Temperature data was collected by the data logger for the complete freeze-thaw cycle.

Average particle sizes of the nanofluids of both concentrations were measured by the Dynamic Light Scattering (DLS) method using a Zeta Potential Analyzer provided by the Brookhaven Instruments Corp [26]. The apparatus was calibrated using the standard aqueous suspension of monodisperse polymer spheres provided by the National Institute of Standards and Technology (NIST). Three samples of the calibration fluid of slightly different concentration were used and five readings for each sample were taken to obtain the final APS. The calibration results showed an APS of 99.9 nm with a standard deviation (σ) of 2.6 nm, which is very comparable to the NIST certified APS of 92 ± 3.7 nm with $\sigma = 7.0$ nm. After this calibration, the apparatus was ready to measure the APS of CuO nanofluids before freezing and after thawing.

Results and Discussion

Three Stages of Cooling

The complete cooling process of a liquid can be divided into three stages: precooling, freezing, and subcooling. These three stages are shown in Figure 2 for deionized water using the data generated from ANSYS Fluent.

(i) Precooling

When the water is cooling from 293.15 K (20°C) to 273.15 K (≈0°C) by heat transfer through 3 thermal resistances: losses to the surroundings (convection and radiation) and conduction through the glass beaker wall and convection on the liquid side. It was determined the precooling stage ended when one of the 29 thermocouples, usually the ones on the periphery (A1, A14, B1, or B14) measured 273.15 K.

(ii) Freezing

The liquid freezes from the periphery towards the center, radially inward, by giving out the latent heat of solidification, until the entire mass is frozen. In this stage of cooling, the heat transfer is occurring from the beaker surface to air by convection and radiation. Under a steady state condition, the same heat is coming from the annular cylindrical ice by conduction and from the liquid in the core region to the inner surface of annular ice cylinder by convection. Therefore, it is a complex problem to theoretically model accurately, unless some simplifying assumptions are made. Freezing was considered complete once the center thermocouple reading reached 273.15K. For a symmetric cooling, usually the last point to freeze will be the center while the periphery may have subcooled.

(iii) Subcooling

During this period the whole solid mass cools below 273.15 K by giving out the contained sensible heat to the beaker wall by pure conduction. The duration for subcooling was determined when the sample reached 264.75 K. This is slightly higher than the set point of 263.15K due to the last part of subcooling is at an asymptotically slower rate as evidence from Figure 2. So, it will take enormously long time of data recording to reach the set point.

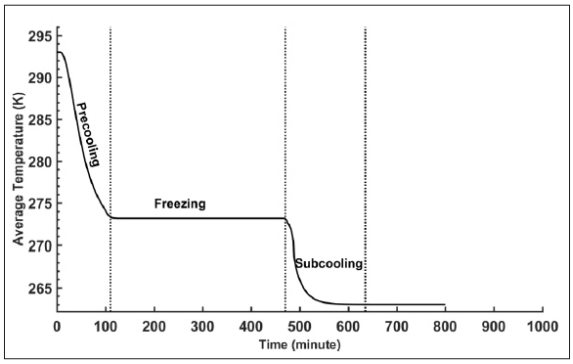

Figure 2: Three cooling stages of water.

Visualization of the Progression of Cooling for D.I. Water

Utilizing the data from all 29 thermocouples, contour plots were generated as shown in Figure 3: (i) at 33 minute during precooling, (ii) at 250 minute when partially frozen and (iii) at 550 minute when subcooled. From the Figure 3, it is observed that the radial cooling occurring in the system is unsymmetrical, although it was expected to be symmetrical cooling. This is due to the thermostatic temperature control system of the thermal chamber. As the internal temperature sensor in the chamber registers an increase in the ambient temperature due to the heat gain from the sample and external air, the thermostat signals to release cold air from the cooling through a vent. This vent is located on the right hand side of the ceiling, releases colder air on the right top quadrant of the beaker. Referring to Figure 1, this area corresponds to location between thermocouples B1 to A14. This area encounters the coldest boundary condition and cools faster.

The freezing begins in this north-east region and advances radially in an unsymmetrical manner toward the south-west region. The contour plots of 1% and 5% CuO nanofluids also exhibited similar progression of unsymmetrical cooling. Thus, the authors used the temperature data located at B1 as a reference point to characterize the cooling of the samples.

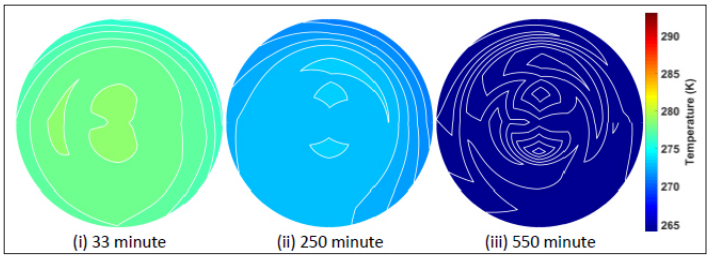

Figure 3: Temperature contours of experimental data at different times exhibiting unsymmetrical
cooling

Cooling Characteristic Curve for D.I. Water

Cooling characteristic curve of deionized water is shown in Figure 4. Due to the selection of a sampling rate of 10 seconds, literally thousands of data points were recorded for the three fluids. However, when all the data points were plotted the curves looked like thick solid lines due to the overlap of symbols. Therefore, to make the Figure 4 and preceding figures clearer, a central line was used to represent all the data while the square symbols are shown at every ≈17 minute intervals.

The first measured data of freezing (reaching 273. 15 K) occurs at 56.7 minutes. The Eq. (1) in ASHRAE is based on the lumped capacitance theory, which can be rewritten into the exponential form shown in Eq. (10), where β is the time constant containing the effects of the fluid properties and total thermal resistance. Using Eq. (10), the precooling and subcooling stages were curve-fitted to determine their respective time constant.

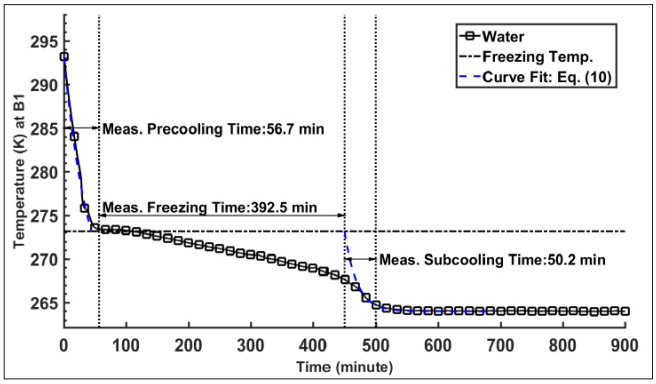

Figure 4: Cooling characteristic curve for water at thermocouple location B1.

$$\frac{T(t)-T_a}{T_i-T_a}=e^{-\beta t}$$

Precooling: $\beta = 4.13\times10^{-4}\,\frac{1}{sec}$ $R^2 = 0.984$ (10)

Subcooling: $\beta \approx 8.5\times10^{-4}\,\frac{1}{sec}$

Then using this value of β, the curve was extended to intersect the 273. 15 K line at the time t = 44.3 minutes. A reasonable agreement between experimental value of 56.7 minutes and the theoretical prediction of 44.3 minutes for reaching the freezing point was observed.

As observed in Figure 4, the duration of freezing or solidification to a complete solid cylinder was measured to take 392.5 minutes.

From Figure 4, it observed the subcooling duration took 50.2 minutes. Then using the curve-fit value of β, the time to subcool to 264.15 K was 45.1 minutes. The agreement between experimental value of 50.2 minutes and the theoretical prediction of 45.1 minutes is reasonable.

Numerical Analysis

In order to obtain comparisons with well-established computational methods, a numerical study using ANSYS Fluent was carried out to derive the times of cooling [27]. For simplicity, a two dimensional model in R and Θ with a constant convective boundary condition around the cylinder was used. Figure 5 shows the meshing of the domain with 1923 elements for the numerical study. A quarter of a circle was used with applying symmetry at the diametric boundaries.

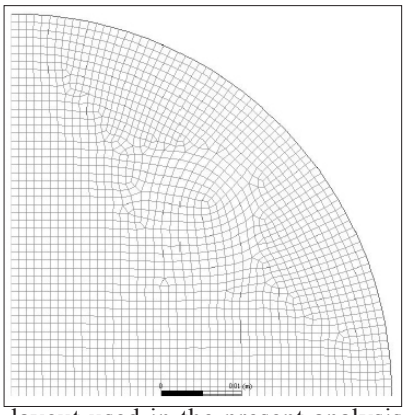

Figure 5: Mesh layout used in the present analysis with 1923 elements.

It was assumed that the liquid in the beaker was stationary (disregarding natural convection); therefore the continuity and momentum equations were not needed for the solution. Using ANSYS Fluent's Solidification & Melting model, the following governing equation was solved for the numerical model. Energy equation with Solidification & Melting model [28]:

$$\frac{\delta}{\delta t}(\rho H)+\nabla\cdot(\rho\vec{V}H)=\nabla\cdot(k\nabla T)+S \qquad (11)$$

Enthalpy

$$H=h+h_f \qquad (12)$$

$$h=h_{ref}+\int_{T_{ref}}^{T}c_p dT \qquad (13)$$

The numerical simulation's initial and Boundary conditions are summarize below:

- Initial temperature was set to 293.15K (matches experimental setup)
- Symmetry was applied to the diametric boundaries.
- Outer wall has a constant heat transfer coefficient that was determined from the curve-fitting of experimental data (Eq. (10)) with an ambient temperature of 263.15K
- The time step size was set to 10 sec (matches experimental setup).

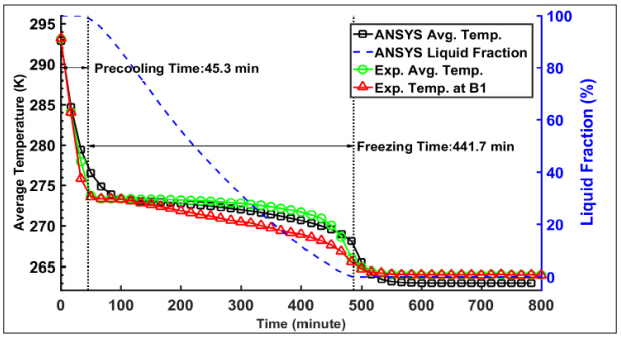

Figure 6: Comparison of ANSYS Fluent results with experimental data

Figure 6 shows the comparison of the three stages of cooling curves for water from experiment and numerical predictions. Despite the difference that the experimental cooling was under unsymmetrical boundary and the ANSYS model is based on symmetrical condition, the comparisons are quite acceptable. The precooling time of 45.3 minutes obtained via ANSYS and the lumped capacitance method is quite good. The experimental average temperatures and the ANSYS average temperatures agree well. The temperature at location B1 subcools earlier as it would be expected compared to the core region thermocouples. For a freeze time of about 441.7 minutes, the liquid fraction goes from 100 to 0%. The magnitudes of cooling times between experiment and the numerical analysis are of similar order of magnitude. Therefore, even with unsymmetrical cooling the experimental setups provides valid data.

Cooling Characteristic Curve for 1% CuO Nanofluid

Cooling characteristic curve of 1% volumetric concentration of CuO dispersed in water is shown in Figure 7. The first measured data of freezing (reaching 273. 15 K) occurs at 57.8 minutes. Using Eq.(14), the precooling and subcooling stages were curve-fitted to determine their respective time constant, β .

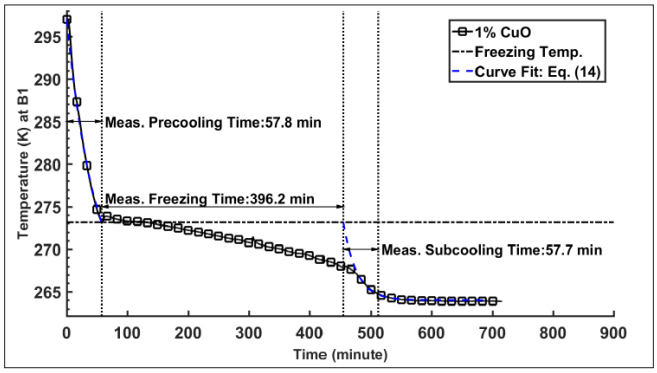

Figure 7: Cooling characteristic curves for 1% volumetric concentration of CuO nanofluid at thermocouple location B1.

$$\text{Precooling: } \frac{T(t)-T_a}{T_i-T_a}=e^{-\beta t} \qquad (14)$$

$$\text{Subcooling: } \beta=3.53\times10^{-4}\frac{1}{sec} \quad R^2=0.9942$$

$$\beta\approx 7.55\times10^{-4}\frac{1}{sec}$$

Then using these values of β, the curve was extended in the precooling region to intersect the 273. 15 K line at the time t = 44.3 minutes.

As observed in Figure 7, the duration of freezing or solidification to a complete solid cylinder was measured to take 396.2 minutes,

Then during the subcooling the frozen mass diminishes in temperature to 263.15 K, which is the set point selected for the Thermotron temperature chamber. From Figure 7, it was observed the subcooling duration to take 57.7 minutes. Similar behavior as depicted in Figure 4 for the thermocouple at location B1 was noticed at other thermocouple locations.

Cooling Characteristic Curve for 5% CuO Nanofluid

Cooling characteristic curve of 5% volumetric concentration of CuO dispersed in water is shown in Figure 6. The first measured data of freezing (reaching 273. 15 K) occurs at 21.8 minutes. This is lower than previous due to start of cooling from an initial temperature of 279.6 K. Using Eq. (15), the precooling and subcooling stages were curve-fitted to determine their respective time constant, β.

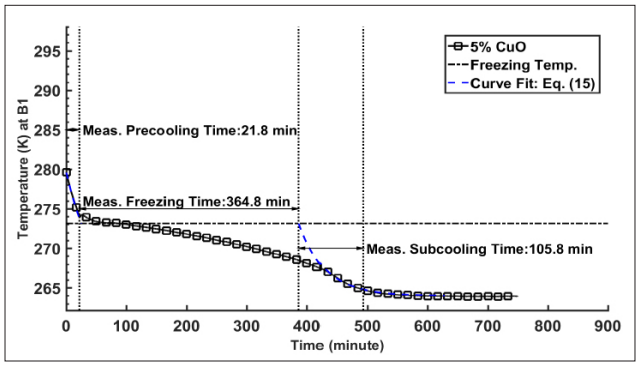

Figure 8: Cooling characteristic curves for 5% volumetric concentration of CuO nanofluid at thermocouple location B1.

$$\frac{T(t)-T_a}{T_i-T_a}=e^{-\beta t}$$

Precooling: $\beta=3.30\times10^{-4}\frac{1}{sec}$ $R^2=0.9993$ (15)

Subcooling: $\beta\approx3.85\times10^{-4}\frac{1}{sec}$

Then using these values of β, the curve was extended in the precooling region to intersect the 273. 15 K line and have an initial temperature of 293.15 K at the time t = 55.5 minutes.

As observed in Figure 6, the duration of freezing or solidification to a complete solid cylinder was measured to take 364.8 minutes,

From Figure 6, we observe the subcooling duration to take 105.8 minutes.

When the nanofluid freezes steadily towards the center there must be convection currents present in the liquid region promoting the transfer of heat from the warmer liquid to the frozen boundary. However, after the entire liquid column has frozen the heat transfer from the core region to the surrounding is by pure conduction.

It is observed that the time to reach the freezing point is longer in case of the nanofluids than water. Also, nanofluid of 5% concentration reaches the freezing point slower than the nanofluid of 1% concentration. This longer subcooling time of nanofluids with higher concentration may be due to the suppression of natural convection current and the coefficient in the liquid due to the presence of heavier nanoparticles.

Comparison of Cooling Time

Table 1 summarizes the times required to undergo the three stages of cooling for water 1% and 5% CuO nanofluids.

Starting from a reference temperature of 293.15 K during the precooling process, water, 1% and 5% nanofluids reached the freezing point in 44.3, 51.9 and 55.5 minutes, respectively. The slower rate of cooling by nanofluids is possibly due to lower natural convection coefficient within the beaker caused by the presence of large agglomerated nanoparticles, which impede the motion. The duration of precooling increases with particle concentration. The times to freeze completely for water (393 min) versus 1 % CuO nanofluid (396 min) are close. Observing the time to freeze for 5% CuO as 365 minutes, it is possible that 1% CuO may localize freezing before 393 minutes. The error is possible due to slight deviations in the experiments. One such case was the placement of the beaker in the camber with respect to the cold air vent. This explanation is based on the fact that the higher concentration nanoparticles have less water, and solid particles do not have a latent heat of solidification and hence the higher concentration nanofluids will require lesser time to freeze. The subcooling time is the shortest for water and longest for nanofluids, increasing with the particle concentration. This could due to the effects of the surfactant.

Table 1: Times for three stages of cooling

Sample	Time in minutes				
	Precooling (Eq. (10),(14),(15))	Freezing (Measured)	Subcooling (Eq. (10),(14),(15))	Time to Freeze	Total Time
Water	44.3	392.5	45.1	436.8	481.9
1% CuO	51.9	396.2	50.8	448.1	498.9
5% CuO	55.5	364.8	99.7	420.3	520.0

A shorter time to freeze completely is a disadvantage of nanofluids, because in case of a heating system failure in a building at subzero temperatures, pipes carrying nanofluids will freeze faster causing bursting of pipes, damage of control valves and circulators and other problems described in ASHRAE handbook [15].

The data in Figures 4, 7 and 8 show all three liquids freeze at about 273.15K. Unlike the results of Hong and Marquis [6] with carbon nanotubes in ethylene glycol, no depression in the freezing point of the base fluid (water) due to the addition of CuO nanoparticles was noticed. A slight variation of 0.1 K to 0.2 K in the freezing point attained by the three fluids is within the precision of Omega type-T (copper-constantan) thermocouple, whose uncertainty is ±0.6 K. Therefore, up to a nanoparticle concentration of 5 %, it was concluded that concentration of nanoparticles did not have any influence on lowering or raising the freezing point of CuO nanofluid in water.

Figure 9 shows how the cooling characteristic curves vary from thermocouple to thermocouple. This figure is a representation of temperature data obtained from four thermocouples at B1, B3, B5 and the center for cooling of deionized water. Being at the periphery, B1 subcools at the fastest rate followed by B3, then B5. The center location temperature goes down from freezing (273.15K) to subcooling (264K) almost vertically in a short period of time than at other thermocouple locations. The central part of the cylinder freezes last. The center freezes by about 440 minutes by which time the peripherally located thermocouple B1 has subcooled to about 268.15 K. Also, the rate of freezing was flatter for thermocouples closer to the center. This is due to the fact that as the freezing front proceeds inward, there is higher thermal resistance for heat to travel from core to the ambient air. Additionally lesser volume material is left at the core whose heat can be extracted in a shorter period of time. After approximately 450 minutes, the subcooling precedes at

the same rate at all thermocouples locations.

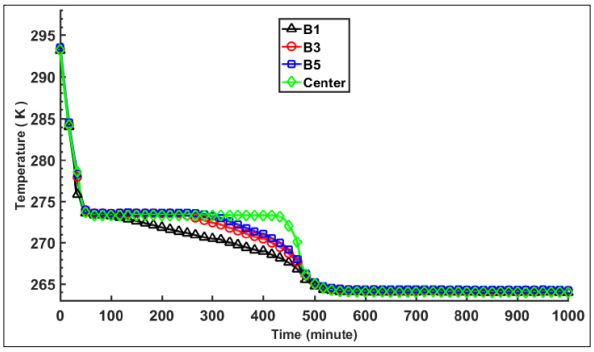

Figure 9: Cooling characteristic curve of deionized water displaying spatial variation from thermocouple locations.

Freeze-Thaw Cycle

Figure 10 & Figure 11 show the complete freeze-thaw characteristic curves for CuO nanofluid of 1% and 5% concentrations respectively. The time of measurement for one complete freeze-thaw cycle was about 1500 minutes or 25 hours. The freezing behavior of the nanofluids is similar to that of water displayed in Figure 9. However, as discussed earlier, the rate of freezing is faster for nanofluids than for water. The thawing process exhibits reverse trend to the freezing characteristics of nanofluids. From both the figures, different rates of freezing and thawing are noticed at the same thermocouple during the complete freeze-thaw cycle. This is due to the differing boundary conditions of 263.15 K during the freezing and 293.15 K during the thawing process.

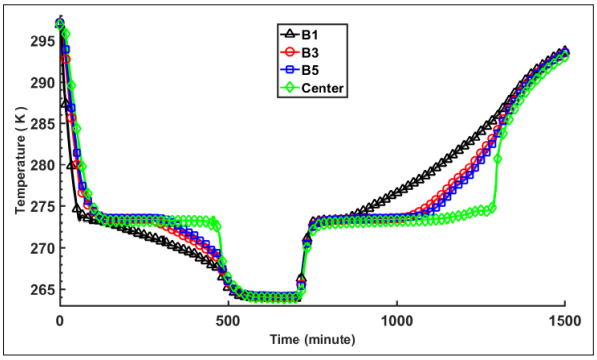

Figure 10: Freeze-Thaw characteristic curve of 1% CuO nanofluid.

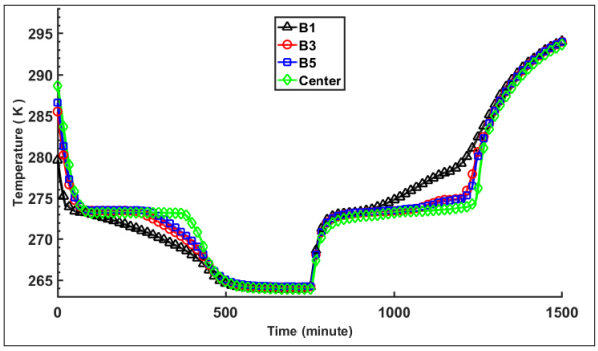

Figure 11: Freeze-Thaw characteristic curve of 5% CuO nanofluid.

Particle Size Measurement

Average particle sizes of the nanoparticles were measured with the DLS method and are summarized in Table 2 for nanofluid samples collected before and after the freeze-thaw cycle. Three samples were collected for both the unfrozen (i.e. before freezing) and thawed (after the freeze-thaw cycle was completed) nanofluid. The unfrozen samples were collected from the nanofluid, which had settled while being stored in the laboratory. The thawed samples were collected: (i) from the bottom of the beaker, (ii) middle of the beaker and (iii) from the top portion (by decantation). Five measurements were taken for each sample and software affiliated with the DLS apparatus produced the average of these readings to yield the final result. The APS of nanoparticles for both the concentrations of settled nanoparticles were comparable with each other; 148 and 164 nm for 1% and 5% concentrations, respectively. They were much higher than the manufacturer-specified size of nanoparticles. This is attributed to the agglomeration of the highly concentrated (50%) original nanofluid settling over a period of nearly one year from the date of procurement.

Table 2: Average particle size distribution for the CuO nanofluid before freezing and after thawing.

	1% CuO		5% CuO	
	APS (nm)	Standard Deviation (nm)	APS (nm)	Standard Deviation(nm)
Before Freezing	147.6	3.6	163.8	1.4
After Thawing	223.2	1.6	239.1	3.7
Difference	51.2 %	NA	46.0 %	NA

Agglomeration due to a single freeze-thaw cycle increases the APS for 1% CuO concentration nanofluid by 51.2%. For 5% CuO concentration nanofluid the increase in APS is 46%. The lesson learned from the particle size measurement is to sonicate adequately the nanofluids, which have been sitting for a while, before charging it to a heat transfer system. After a freeze-thaw cycle, sonication and particle size measurement must be conducted to ascertain that the manufacturer specified APS is achieved. Going from 1% to 5% concentration did not significantly increase the agglomerated particle size; from 223nm to 239 nm a mere 7% increase. If a nanofluid experiences multiple freeze-thaw cycles, the APS would increase by a higher percentage. It is advisable to subject the thawed nanofluid to high level of ultrasonication to ascertain that the agglomerated nanoparticles have broken down to the pre-freeze average particle size.

Conclusion

Freeze-thaw characteristics of 1% and 5% volumetric concentrations of the copper oxide nanofluid in water were studied via experiments. Results showed no lowering of the freezing point, as observed in the saline water, of the nanofluid due to the addition of nanoparticles, as high as 5 % concentration. Precooling time took longer for nanofluids and increased with higher volumetric concentration of nanoparticles. To freeze fully, the 5% nanofluids took shorter time than water and the 1% nanofluid. Agglomeration due to a single freeze-thaw cycle increased the APS by about 46-50% than the unfrozen sample. Concentration did not seem to affect significantly the size of the agglomerated particle over a single freeze-thaw cycle. After thawing, ultrasonication is absolutely necessary to break down bigger nanoparticles and hence result in efficient recycling of nanofluids in thermal applications.

Acknowledgement

The assistance of Prof. Thomas Trainor of Chemistry Department in the use of DLS apparatus and Prof. Rorik Peterson of Mechanical Engineering Department in the use of Thermotron Programmable Temperature chamber is gratefully acknowledged.

References

1. Vajjha RS, Das DK (2009) "Experimental determination of thermal conductivity of three nanofluids and development of new correlations". International Journal of Heat and Mass Transfer 52: 4675-4682.
2. McQuiston FC, Parker JD, Spitler JD (2005) Heating, ventilating, and air conditioning: analysis and design, John Wiley & Sons.
3. Strandberg R, Das DK (2009) "Hydronic Coil Performance Evaluation with Nanofluids and Conventional Heat Transfer Fluids". Journal of Thermal Science and Engineering Applications 1: 011001-011001.
4. Strandberg R, Das DK (2010) "Finned tube performance evaluation with nanofluids and conventional heat transfer fluids". International Journal of Thermal Sciences 49: 580-588.
5. Ray DR, Das DK (2014) "Superior Performance of Nanofluids in an Automotive Radiator". Journal of Thermal Science and Engineering Applications 6: 041002-041001 to 041002-041016.
6. Hong H, Marquis FDS (2007) "Carbon naoparticle-containing hydrophilic nanofluid," Google Patents.
7. Chon CH, Kihm KD, Lee SP, Choi SUS (2005) "Empirical correlation finding the role of temperature and particle size for nanofluid (Al_2O_3) thermal conductivity enhancement". Applied Physics Letters 87: 153107.
8. Koo J, Kleinstreuer C (2005) "A new thermal conductivity model for nanofluids". Journal of Nanoparticle Research 7: 324-324.
9. Boutine C (2001) "Taking the heat off: Nanofluids promise efficient heat transfer". logos 19.
10. Ivall J, Hachem M, Coulombe S, Servio P (2015) "Behavior of Surface-Functionalized Multiwall Carbon Nanotube Nanofluids during Phase Change from Liquid Water to Solid Ice" Crystal Growth & Design 15: 3969-3982.
11. Das SK, Choi SUS, Yu W, Pradeep T (2008) Nanofluids: Science and Technology, Wiley, Hoboken, NJ.
12. Minkowycz WJ, Sparrow EM, Abraham JP (2013) Nanoparticle Heat Transfer and Fluid Flow, CRC Press/Taylor & Francis Group, Boca Raton, FL.
13. Maré T, Sow O, Halelfadl S, Lebourlout S, Nguyen CT (2012) "Experimental Study of the Freezing Point of γ-Al2O3/Water Nanofluid". Advances in Mechanical Engineering 4: 162961.
14. Lunardini VJ (1981) Heat transfer in cold climates, Van Nostrand Reinhold Co.
15. American Society of Heating, R., Engineers, A.-C., and Ashrae, 2013, 2013 ASHRAE Handbook: Fundamentals, ASHRAE.
16. Plank R (1941) Beiträge zur Berechnung und Bewertung der Gefriergeschwindigkeit von Lebensmitteln, VDI-Verlag.
17. Pham QT (1984) "Extension to Planck's equation for predicting freezing times of foodstuffs of simple shapes". International Journal of Refrigeration 7: 377-383.
18. Cleland AC, Earle RL (1979) "A Comparison of Methods for Predicting the Freezing Times of Cylindrical and Spherical Foodstuffs". Journal of Food Science 44: 958-963.
19. Kotz JC, Treichel PM, Townsend J (2012) Chemistry and Chemical Reactivity, Cengage Learning.
20. Boyd CE (2015) "Physical Properties of Water". Water Quality: An Introduction, Springer International Publishing Cham 1-19.
21. Alfa Aesar (2013).
22. Brason Ultrasonics Corporation (2008).
23. Thermotron Benchtop Temperature Chambers 2008.
24. National Instruments (2017) "National Instruments".
25. National Instruments (2017) "Introduction Labview".
26. Brookhaven Instruments Corporation (2017) "90 Plus Size Analyzer".
27. ANSYS Academic Reasearch Release (2017) "Fluent Academic Research, Release 18.1."
28. ANSYS Academic Reasearch Release (2017) "ANSYS Fluent Theory Guide 18.1."